Claudia Rentsch, Wolfgang Schneiders, Ricarda Hess, Barbe Rentsch, Ricardo Bernhardt, Kathrin Spekl, Konrad Schneider, Dieter Scharnweber, Achim Biewener, Stefan Rammelt

Healing properties of surface-coated polycaprolactone-co-lactide scaffolds: A pilot study in sheep

Erstveröffentlichung in / First published in:

Journal of Biomaterials Applications. 2014, 28(5), S. 654 - 666 *[Zugriff am: 31.07.2019]*. SAGE journals. ISSN 1530-8022.

DOI: https://doi.org/10.1177/0885328212471409

JOURNAL OF
biomaterials applications

Article

Journal of Biomaterials Applications
2014, Vol 28(5) 654–666

DOI: 10.1177/0885328212471409
jba.sagepub.com
SAGE

Healing properties of surface-coated polycaprolactone-co-lactide scaffolds: A pilot study in sheep

Claudia Rentsch[1,2], Wolfgang Schneiders[1,2], Ricarda Hess[3], Barbe Rentsch[4], Ricardo Bernhardt[3], Kathrin Spekl[5], Konrad Schneider[6], Dieter Scharnweber[3,7], Achim Biewener[1,2] and Stefan Rammelt[1,2,7]

Abstract

The aim of this pilot study was to evaluate the bioactive, surface-coated polycaprolactone-co-lactide scaffolds as bone implants in a tibia critical size defect model. Polycaprolactone-co-lactide scaffolds were coated with collagen type I and chondroitin sulfate and 30 piled up polycaprolactone-co-lactide scaffolds were implanted into a 3 cm sheep tibia critical size defect for 3 or 12 months ($n = 5$ each). Bone healing was estimated by quantification of bone volume in the defects on computer tomography and microcomputer tomography scans, plain radiographs, biomechanical testing as well as by histological evaluations. New bone formation occurred at the proximal and distal ends of the tibia in both groups. The current pilot study revealed a mean new bone formation of 63% and 172% after 3 and 12 months, respectively. The bioactive, surface coated, highly porous three-dimensional polycaprolactone-co-lactide scaffold stack itself acted as a guide rail for new bone formation along and into the implant. These preliminary data are encouraging for future experiments with a larger group of animals.

Keywords

Polycaprolactone-co-lactide scaffold, collagen type I and chondroitin sulfate, sheep, tibia defect, bone healing

Introduction

Current clinical options in the treatment of critical size bone defects due to trauma, inflammation, and tumor resection are limited, and pose a continuous challenge in orthopedic surgery. Although autogenic and allogenic bone grafting are established clinical methods, none of these techniques is optimal in terms of hospitalization time, stability, storage, immune reaction, infection risk, pain, and availability.[1,2]

Actual investigations of new bone implants using different biomaterials, such as hydroxyaptite, polymers, metals, and composites,[3–5] partly in combination with growth factors,[6] platelet-rich plasma, bone marrow, mesenchymal stem cells,[7–9] or gene therapy,[10,11] have been proposed as alternatives, but until now only a few of the unconventional bone graft techniques have been incorporated into the clinical setting.[12–14]

Biocompatible and resorbable polymers like poly(ε-caprolactone) and poly(lactic acid) and their copolymers, are promising materials for biomedical applications in bone and cartilage repair[15,16] drug delivery systems[17] and as surgical sutures.[18]

In addition to the graft itself, the extracellular matrix (ECM) plays an important role for bone forming and bone resorbing cells in controlling development, maintaining homeostasis, and guiding regeneration. Type I

[1]Department of Trauma and Reconstructive Surgery, University Hospital Carl Gustav Carus Dresden, Dresden, Germany
[2]Centre for Translational Bone, Joint and Soft Tissue Research, University Hospital Carl Gustav Carus Dresden, Dresden, Germany
[3]Max Bergmann Center of Biomaterials, Dresden, Germany
[4]Catgut GmbH, Markneukirchen, Germany
[5]Medical Theoretical Center, Dresden, Germany
[6]Department of Mechanic und Structure, Leibniz Institute of Polymer Research Dresden e.V., Dresden, Germany
[7]DFG-Center for Regenerative Therapies Dresden, Dresden, Germany

Corresponding author:
Claudia Rentsch, Department of Trauma and Reconstructive Surgery, University Hospital Carl Gustav Carus Dresden, Fetscherstrasse 74, 01307 Dresden, Germany.
Email: claudia.rentsch@uniklinikum-dresden.de

collagen (coll I), the key organic structure of the ECM, can be immobilized to the surface of implants, maintaining its structural properties and creating an artificial ECM. The positive effects of coll I on bone remodeling[19,20] can be further enhanced by adding glycosaminoglycans like chondroitin sulfate (cs). CS is used in matrices in combination with coll I as a structural component in tissue regeneration.[21–25]

The aim of this pilot study was to investigate the healing properties of coll I/cs coated polycaprolactone-co-lactide (PCL, trade name; Catgut GmbH, Markneukirchen) scaffolds using a large animal model. The three-dimensional scaffold stack (composed of 30 single scaffolds) was implanted in a 3 cm tibiae critical size defect in sheep. New bone formation was determined over a period of 3 and 12 months by histological, radiological, computer tomographical (CT), and biomechanical investigations.

Material and methods

Production and coating of PCL scaffolds

The copolymer of L-lactide and ε-caprolactone (75/25) was melt spun and resulted in a synthetic, resorbable, monofilament fiber, available as PCL suture (Catgut GmbH, Germany). A traditional manufacturing technique (embroidery) was used to produce the scaffolds presenting a triaxial structure (deposition of the thread in a triangular assembly; 0/60/120 netting) with a stitch length of 1.4 mm and a mesh spacing of 1.2 mm. The resulting round, textile scaffolds with 19 mm outer and 10 mm inner diameter had a height of *ca* 1 mm (Figure 1(a)). These scaffolds can be piled up, depending on the defects size, to create a real three-dimensional implant (Figure 1(c)).

The coll I/CS matrix coating was produced as previously described.[22] Porcine skin coll I (MBP GmbH, Neustadt-Glewe, Germany) was suspended in 0.01 M acetic acid, diluted in phosphate buffer (60 mM Pi, 270 mM NaOH, pH 7.4) with 1.25 mg/mL CS A and B (Sigma–Aldrich, St. Louis, MO) to 2.5 mg/mL. After scaffold coating, a cross-linking step followed by adding 0.1 M N-(3-dimethylaminopropyl)-N′-ethylcarbodiimide hydrochloride and 0.05 M N-hydroxysuccinimide (Sigma–Aldrich, St. Louis, MO) in 0.1 M phosphate buffer at pH 5.5/40% ethanol.

Microcomputer tomography of the scaffold

The general porosity and the pore-size distribution of the three-dimensional scaffold stack were determined using non-destructive microcomputer tomography (μCT) analysis with the Scanco vivaCT 75 system (Scanco Medical, Brüttisellen, Switzerland). The samples were measured with radiological energy of 55 keV and 1500 projections. The voxel resolution of the reconstructed volume was 20 μm. The porosity and the pore size distribution were measured with the Scanco evaluation software.

Surgical procedure

This study has been licensed by the regional veterinary board (24D-9168.11-1-2006-17). All animals were cared for according to the European guidelines for the care and use of laboratory animals (Directive 24.11.1986, 86/609/CEE).

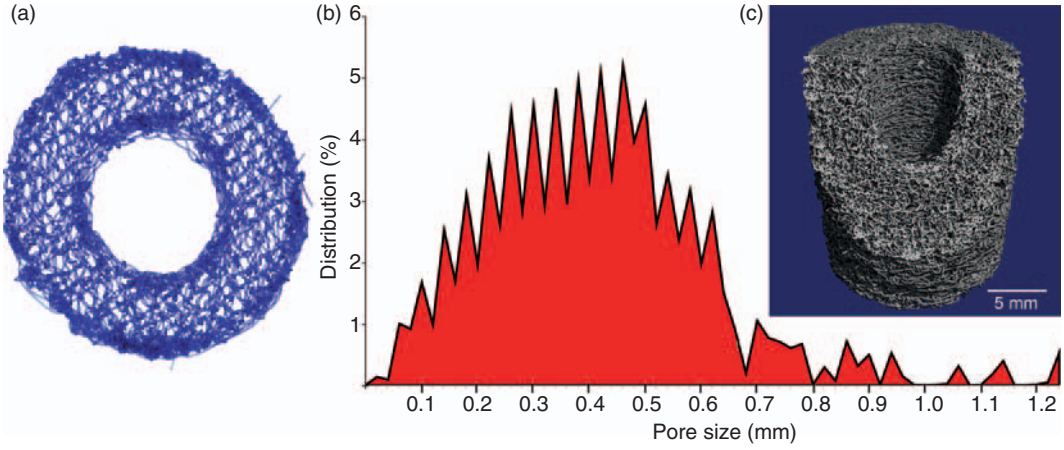

Figure 1. PCL scaffold: (a) embroidered, single PCL scaffold, the 10 mm inner space was prepared to allow the piling around the marrow nail, (b) pore size distribution of the implant, and (c) presentation of the three-dimensional scaffold stack composed of 30 single PCL scaffolds.
PCL: polycaprolactone-co-lactide.

A total number of 10 female sheep with an average body weight of 65 kg was used for this study. Animals achieved an intramuscular (IM) premedication of xylazine (Rompun®, Bayer, Germany, 0.9 mg/kg body weight) as well as a prophylactic amoxicillin antibiotic therapy (Duphamox, Pfizer AG, Zürich, Switzerland, 15 mg/kg body weight) prior to surgery. Surgery was carried out in a lateral decubitus position under general anesthesia (induced with sodium thiopental and maintained via inhalation of a mixture of nitrous oxide and 2% isoflurane).

A 3 cm long mid-diaphyseal segment was removed from the left tibia of each sheep. The defect was stabilized by a 20 cm long prototype tibial nail (UTN, Clinical House GmbH, Bochum, Germany). For the insertion of the nail, a longitudinal incision was made over the knee and the patellar tendon was split in the middle. An inlet hole was created at the level of the tibial tuberosity. The nail was inserted without previous reaming of the medullary canal through the tibia head, while the diaphysis was osteotomized with an air-oscillating saw through an anteromedial incision 6 cm below the knee joint (Figure 2(a) and (b)). The 3 cm bone segment was removed with the periosteum and replaced with a Rebofacin® Bone Cement R spacer (Biomet GmbH, Ried, Switzerland), molded by hand to the shape of the resected bone part (Figure 2(c)). The surgical field was constantly washed with sterile phosphate buffer saline (PBS) while the bone cement polymerized. All nails were locked proximally and distally with two locking screws of 40 mm length and 4 mm diameter (Synthes GmbH, Umkirch, Germany). To reduce weight bearing on the operated leg, the achilles tendon was cut percutaneously. Subcutaneous tissue and skin were closed using MARILIN and MARIDERM suture material (Catgut GmbH,

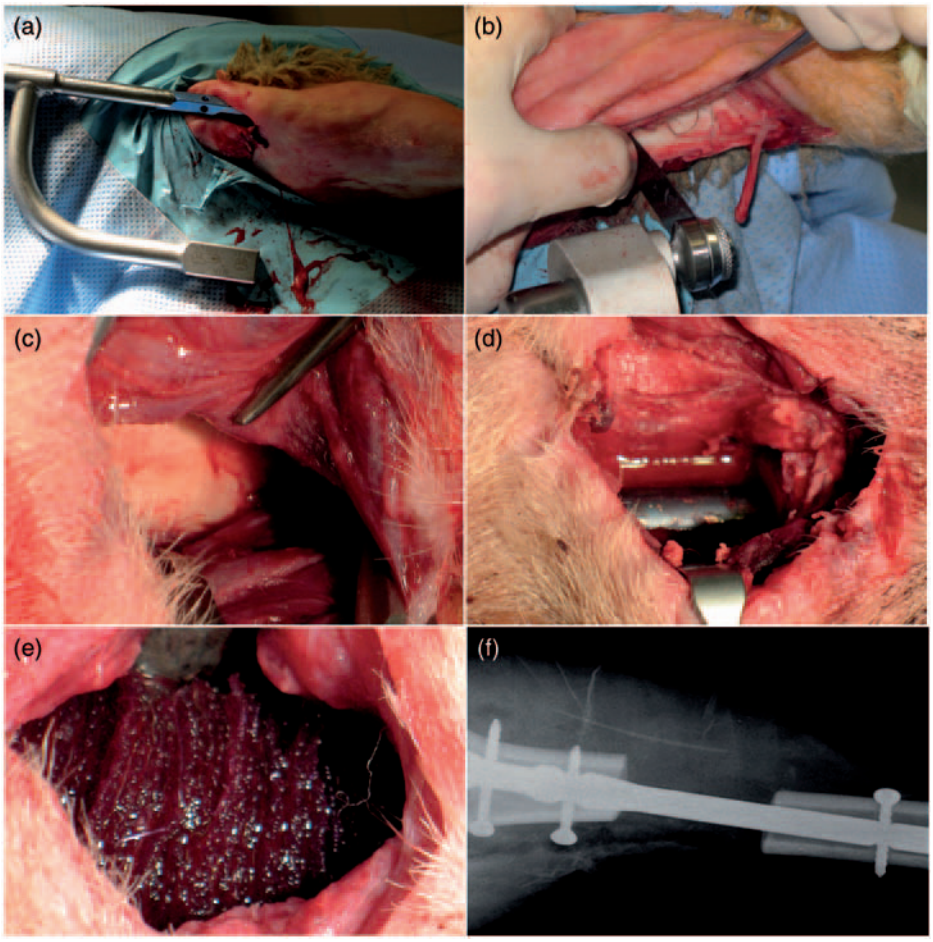

Figure 2. Surgical procedure: (a) insertion of the 20 cm long prototype tibia nail, (b) osteotomy of the tibia mid-diaphysis using an air-oscillating saw, (c) Rebofacin® Bone Cement R spacer filled the 3 cm defect size for 6 weeks, (d) removed bone cement, proximal and distal tibia end visible as well the marrow nail, (e) 30 inserted coll I/CS scaffolds and (f) final X-ray control (PCL scaffolds are not detectable at radiographs).
coll I/cs: Type I collagen/chondroitin sulfate; PCL: polycaprolactone-co-lactide.

Markneukirchen, Germany) under routine procedures. Six weeks later, a 6 cm incision was made at the diaphysis orientated at the previous scar and the bone cement was carefully removed (Figure 2(d)). Finally, the defect was filled with 30 coll I/CS scaffolds for 3 or 12 months (Figure 2(e)). For that, the single scaffold discs were cut open on one side, thread around the marrow nail and piled up until the defect was completely filled.

Pain control was managed by 75 mg carprofen (Rimadyl, Pfizer AG, Zürich, Switzerland) IM, and antibiotic prophylaxis was carried out through three subsequent doses of 150 mg Duphamox IM. Animals were euthanized after 3 or 12 months with a lethal dose of T-61 (Hoechst Roussel Vet, Wiesbaden, Germany). Screws and nail were removed directly after tibia preparation.

Radiography

Radiographs were taken with a mobile X-ray unit (AMX 4, GE Healthcare, Buckinghamshire, UK) using 52 kV and 2.5 mAs.

Computer tomography

Explanted tibiae of the 3-month group were assessed for apparent bone mineral density with a CT scanner (SOMATOM Sensation 16, Siemens Medical Solutions USA, Inc., Malvern, PA). The scan was done using a high-resolution bone window level setting tomography with 120 kV, 166 mA. The images were reconstructed with 0.6 mm thick slices using SIENET MagicView 300 analyzing software (Siemens, Erlangen, Germany). CT scans were quantified for new bone formation in the defect zone. The defect area was visually localized between lateral and distal intact cortical bone.

μCT Analysis of the tibia (12-month group)

Explanted tibiae of the 12-month group were assessed with a non-destructive μCT analysis using the Scanco vivaCT 75 systems (Scanco Medical, Brüttisellen, Switzerland). The samples were measured with radiological energy of 70 keV and 500 projections. The voxel resolution of the reconstructed images was 70 μm. The new bone volume within the defect area was measured with the Scanco evaluation software.

Histology

Explants were fixed in 4% buffered formalin for at least 7 days.

Three-month group: The defect area was localized by measuring the distance between proximal and distal locking screw and the visible callus formation. The defect zone was cut in seven equal section planes of 0.5 cm, beginning and ending beyond the implant area. Each section plane was separated into quarters to fit the embedding cube. The samples were washed, decalcified for 4 weeks in ethylenediaminetetraacetic acid (to adjust pH to 7.4–7.6 use NaOH), dehydrated overnight in a Shandon Hyper Center tissue processor (Rankin Biomedical Corp., Clarkston, MI), and embedded in methylmetacrylate (Technovit 9100 New, Heraeus Kulzer GmbH, Werheim, Germany) according to manufacturer instructions. Sections of 3 μm were cut (rotation microtome RM2055, Leica Microsystems, Wetzlar, Germany), methylmethacrylate was removed using xylene for 2×20 min, 2-methoxyethylacetat for 2×20 min, acetone for 2×5 min, and 80% ethanol, and stained for light microscopy (Leica DMRBE Research Microscope, Camera Leica DC300, Leica Microsystems, Wetzlar, Germany). Presented images were taken from the central part of the 3 cm defect area.

Twelve-month group: The samples of the 12-month group (after biomechanical testing) were dehydrated overnight and embedded in methylmetacrylate according to manufacturer instructions. Special glass slides ($5 \times 10\,cm^2$, Langenbrinck Labor- und Medizintechnik, Emmendingen, Germany) were used to allow the application of the longitudinal-sectioned defect zone. Sections of 10 mm were obtained with the Exakt cutting and grinding equipment (Exakt, Norderstedt, Germany) and stained for light microscopy.

Masson–Goldner trichrome staining. Samples were stained with Ponceau acid fuchsin for 5 min, wash in acetic acid, 1% and place in acid-Orange G solution. Rinse in acetic acid, 1% for 30 s and stain in light green for 5 min. Rinse in acetic acid, 1%, for 5 min and counter stain by hematoxylin staining according to Weigert (15 min).

Modified Masson–Goldner trichrome staining. Trichrome staining according to Masson–Goldner combines Ponceau (5 min), Orange G (5 min), and anilin blue tartrazine solution (15 min). Tartrazine stains collagen structures in yellow and in combination with anilin blue which also stains collagen, the final coloring results are various shades of green to yellow.

Sections were always washed with 3% acetic acid between every staining step. Nuclei (brown) were counter stained by hematoxylin staining according to Weigert (15 min).

1A4-Actin staining. For immunohistology, 3 μm sections were incubated with the primary antibody (mouse anti-human smooth muscle Actin, clone 1A4, DAKO, Glostrup, Denmark) overnight at 4°C, than incubated

with biotin conjugated bridging antibody 1:150 in blocking solution (1% BSA in PBS, 30 min, 37°C) and finally incubated in avidin-biotin conjugated peroxidase (Vectastain universal Elite Kit, Vector Laboratories, Burlingame, CA) for 30 min. The immune reaction was visualized with Romulin (Biocare Medical, Concord, CA) for 15 min at room temperature. Sections were counterstained with hematoxylin (Merck, Darmstadt, Germany; 5 min). Samples incubated without primary antibody were used as control.

Biomechanical testing

The explanted tibiae of the 12-month group were fixed to a biomechanical universal testing machine (TIRA test 2300, Schalkau, Germany). A three-point bending test was conducted using 2 N pre-load and a test loading speed of 10 mm/min until the fracture occurred. The contralateral tibiae were used as a reference. The maximum load until failure and the stiffness (dividing the load at failure by the displacement at failure) were calculated and compared to the control group.

Results

μCT of the PCL scaffold stack

Figure 1(c) shows a three-dimensional reconstruction of the μCT analysis of the PCL scaffold stack, which represents the implant for the 3 cm critical size defect in the sheep tibiae. The stack showed a homogeneously distributed interconnected porosity of 87% and a main pore size range of 0.1–0.8 mm distributed over the whole stack (Figure 1(b)).

Complications

Two animals of the 12-month group sustained a tibial shaft fracture after nail insertion and had to be fixed with a cerclage wire.

During the entire course of the experiment, two hardware failures occurred (each in one group). The animals showed a broken intramedullary nail at the 6-week radiographic control and were excluded from further analysis.

Radiography, CT and histology at 3 months

There was no callus formation detectable after 6 weeks of bone cement implantation (X-ray not shown). Six weeks after scaffold implantation, an initial callus reaction was seen around the implants during radiological control X-rays. In all animals, the callus reaction occurred at both the proximal and distal part of the tibia.

Both the radiographs and the CT analyses at 3 months demonstrated new bone formation predominately at the posterior aspect of the tibia, opposite to the site of surgery and close to the flexor muscles of the lower leg (Figure 3(a) and (b)).

The PCL scaffold was still visible at 3 months after implantation (Figure 3(c)) and completely intermingled with connective tissue, firm connective tissue, cartilage, and bone. New bone formation was mostly localized at the peripheral zone of the scaffold stack. Small islets of new bone matrix were present at the inner parts of the scaffolds straight around the scaffold fibers. The new bone matrix enclosed the scaffold fibers without any fibrous interface (Figure 3(d) and (e)). No inflammatory reaction was visible around the implant material after 3 months. 1A4 Actin staining proved complete vascularization of the scaffold (Figure 3(f)).

Quantification of the bone volume ratio at 3 months

Based on the CT quantification of newly produced bone volume in the defect zone, new bone formation in all four animals reached an average of 63% (+/−37%). Two of four sheeps (Figure 5) showed almost 100% of new bone mass within the defect zone whereas the other two animals revealed substantially less (28% and 34%). CT quantification of a 3 cm midshaft bone segment of the contralateral tibiae was used as reference value (100%).

Radiography and μCT at 12 months

The 12-month radiographs and μCT scans revealed that two out of four tibial defects were bridged completely. Most of the new bone was seen opposite to the site of surgery. New bone formation occurred from both the proximal and distal bone ends toward the defect. One out of four animals showed a hypertrophic nonunion (Figure 4(b)) and one an atrophic nonunion (Figure 4(d)). Both animals presenting a nonunion after 12 months had to be stabilized with a cerclage wire after nail insertion during surgery (see radiograph in Figure 4(d)).

Quantification of the bone volume ratio at 12 months

Based on the μCT quantification of the 12-month group, the newly formed bone averaged 172% (+/−86%) as compared to the intact contralateral tibiae used as a reference value (100%; Figure 5). The total bone volume averaged 12,262 mm^3 (+/−6148 mm^3) within the defect area compared to 7194 mm^3 (±1008 mm^3) bone at the reference site. One animal (number 3 in Figure 5) showed substantially less

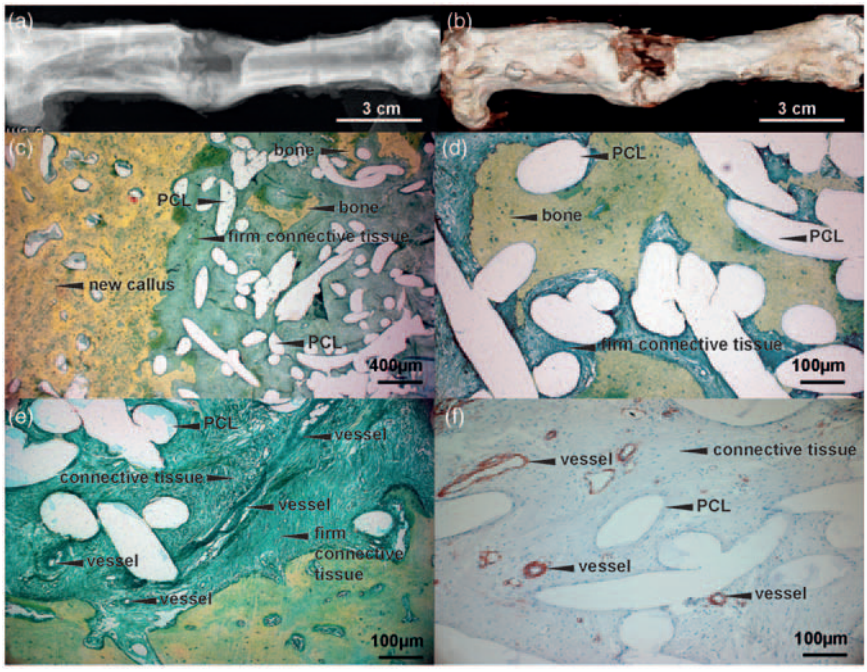

Figure 3. Radiography, computer tomography and histology at 3 months. (a) to (d) presents the data of the animal with the highest new bone formation in the 3 month group. The intramedullary nail and screws were removed after explantation. (a) x-ray of a sheep tibia; (b) 3 dimensional CT reconstruction of a sheep tibia; (c) to (e) present images of modified Masson-Goldner Trichrome staining. (c) histological cross section was taken of the central defect part, new bone formation occurred mainly at the outer scaffold part; (d) histological cross section of the central defect part, inner scaffold area showed small islets of new bone formation; (e) The scaffold was completely intermingled with vascularized, connective and firm connective tissue showing a new bone formation around scaffold fibres; (f) 1 A4 Actin staining proved complete vascularization of the scaffold.

(43%) new bone compared with the other three of this group (215% (+/−9%)).

Biomechanical estimation at 12 months

The average maximum load until failure of the non-operated tibiae averaged 5875 N (±559 N). Two operated tibiae reached 49% (2880 N) and 63% (3720 N) of the reference value for normal bone, respectively (Figure 6(a)). The values in the other two animals were in a lower range of 18% (1050 N) and 7% (428 N).

The average stiffness of the contralateral tibiae averaged 387 N/mm (±33 N/mm; Figure 6). Two of four animals reached a maximum stiffness of 46% (179 N/mm) and 40% (155 N/mm) of the control value, whereas, the other two animals reached only 20% (82 N/mm) and 4% (16 N/mm) of the stiffness of the contralateral tibiae (Figure 6(b)).

Physiological and histological evaluation at 12 months

New bone formation was observed macroscopically in all explants. After longitudinal sectioning of the tibiae, the scaffold zone was still detectable (Figure 7(b)). The implant was completely integrated into newly formed bone. Most of the bone was seen at the posterior aspect of the tibia, opposite to the site of surgery. The new bone matrix enclosed the scaffold fibers without any fibrous interface.

Histological staining revealed a new bone formation at both the proximal and distal bone ends within and outside the scaffold-stack. Fibrous tissue and cartilage were seen as well (data not shown). The scaffold was completely vascularized and erosion of the PCL-fibers was clearly visible. No inflammatory reaction was evident around the implant material after 12 months.

Discussion

Previous studies using embroidered scaffolds in other model systems demonstrated that they can act as a temporary structure for cell migration, proliferation, and differentiation in vitro and in vivo. The use of ECM components like coll I/CS-enhanced osteogenic differentiation and bone matrix accumulation.[16,22,26] The aim of this study was to evaluate the healing properties of coll I/CS-coated PCL scaffolds in a large animal

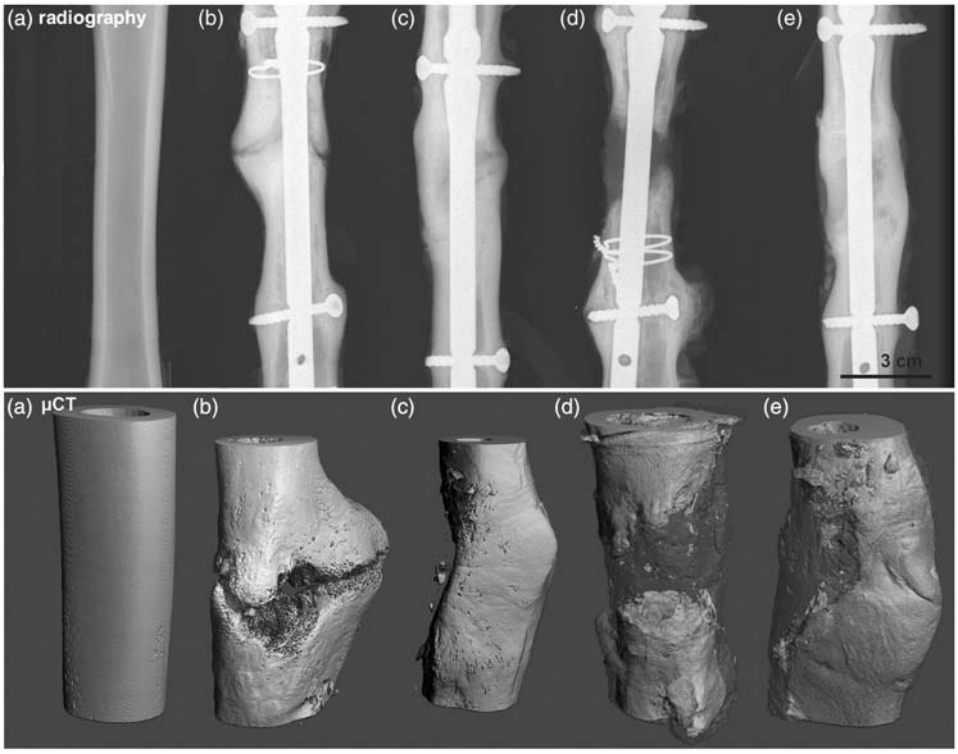

Figure 4. Radiography and CT at 12 months: (a) control tibia, (b) hypertrophic nonunion, (c) bridged defect, (d) atrophic nonunion, and (e) bridged defect. The intramedullary nail and screws are visible in the radiographs of the operated tibiae (top row), for CT analysis, the intramedullary nail and screws had been removed (bottom row).
CT: computer tomography.

pilot study. A critical size defect in the sheep tibia was filled with a three-dimensional scaffold and investigated after 3 and 12 months.

Surgical procedure

The two-step surgery according to Masquelet[27] and Viateau et al.[9] seemed to be appropriate to form a vascularized, fibrous tissue ('periost-like membrane') surrounding the defect area after 6 weeks and represents a clinically relevant model. The mechanical stabilization is achieved in a first step whereas the tissue engineering is employed in a second step after eradication of an infection treatment or resection/irradiation of a tumor. Because the periosteum was completely removed within the defect region, the observed new bone formation seems to have been generated in part by the 'periost-like membrane'.

The critical size defect of 3 cm and the intramedullary nail fixation were selected based on literature data.[8,23,28–30] Although all animals had the same age and weight, the tibia size differed and thus altered the fitting of the single-sized intramedullary nail. Additional fractures, treated with a cerclage, and probably unknown microfractures may be responsible for the considerable variation of the presented results including a hypertrophic and atrophic nonunion. Concluding, the stability of the osteosynthesis in this pilot study seems insufficient.

A total of 2 out of 10 animals displayed a broken marrow nail at the 6 weeks X-ray control (after implantation of the PCL scaffold) and were excluded from the experiment. It is supposed that the hardware failure occurred during uncontrolled full weight bearing by the animals. Both, Reichert et al.[31] and Hahn et al.[32] described complications occurring during full weight bearing involving peak loads during laying down and standing up.[31,32] However, all described mechanically fixation systems in animal models, like intramedullary nailing, external fixation, or plate fixation have potential disadvantages like thermal necrosis, reduced intraosseous blood flow, infection or hardware loosening.[31,32] Recently, a low contact dynamic compression plate has been suggested for further experiments.[32]

Bone quantification

Bone quantification was performed using CT (3-month group) and µCT (12-month group). The current pilot study revealed a mean new bone formation of 63% and 172% after 3 and 12 months, respectively. To estimate the value of new bone formation using coll I/CS coated

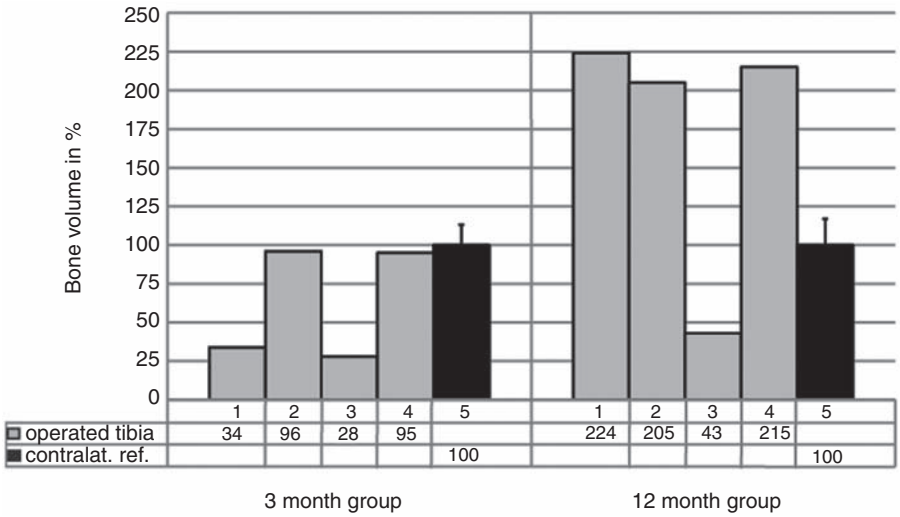

Figure 5. Quantification of the bone volume ratio at 3 and 12 months.
The calculated amount of calcified matrix in each animal is depicted in gray bars. The 3 cm midshaft segments of the contralateral tibiae (contralateral reference) were used as reference area (black bars, mean value including standard deviation).

PCL scaffolds, these numbers were compared to that of nine relevant large animal studies (Table 1).

All of these studies expressed the final amount of newly formed bone as a percentage of normal bone and therefore seemed to be appropriate for comparison. In summary, the published reports indicate that implants without cells formed approximately 17% of new bone. Empty controls showed a mean bone volume of 13% and controls with autologous bone grafting, a mean bone volume of 46% (Table1). Most large animal studies offer observation periods of 12 or 16 weeks and only two of them up to 6 months. Compared to the available data from the literature, this pilot study presents a higher amount of new bone formation in the 3-month group than any other investigated scaffold in large animal experiments. With an average amount of 63% of new bone after 3 months, this study surpasses the values of that with autologous bone grafting (46%) from the literature. Mastrogiacomo et al.[40] describe one of the rare long-term studies for critical size bone defects in large animals. They investigated five sheep for 12 months using resorbable bioceramics based on silicon-stabilized tricalcium phosphate. The authors achieved around 60% of new bone after 12 months analyzing microradiograph sections, which is considerably less than in this study with two fully bridged defects showing around 220% of new bone formation. This large amount of bone originates from the strong callus formation within the defect area. The lower bone formation in the study by Mastrogiacomo et al.[40] could have been due to the larger defect size of 4.8 cm. All comparisons have to be interpreted with caution considering the different study designs and the small number of animals in the present pilot study.

Biomechanics

The quantity of the newly formed bone is not the only important factor in bone healing. The bone quality, including cortical and trabecular structure, thickness and porosity provide evidence for the apparent mechanical properties.[41] The measured biomechanical stability (load to failure) of 63% and 49% in the two bridged defects compared to the non-operated tibia after 12 months are encouraging for planning further animal studies using a greater number of animals. It is difficult to interpret the obtained data because no relevant biomechanical studies in large animals are available. They may, however, serve as a reference for future experiments.

Histological evaluation

A highly osteogenic activity was seen in connective tissue–bone interfaces next to bone–cartilage interfaces which points to endochondral and intramembraneous ossification in healing of a critical size bone defect. Endochondral ossification (soft callus remodeling) represents a typical fracture healing stage according to the four-stage model.[42] All histologically stained sections present the third stage (hard callus formation) of the fracture healing according to Schindler et al.[42]

The scaffold was completely intermingled with vascularized connective tissue, showing bony islets around the PCL fibers at the inner part of the scaffold after 3

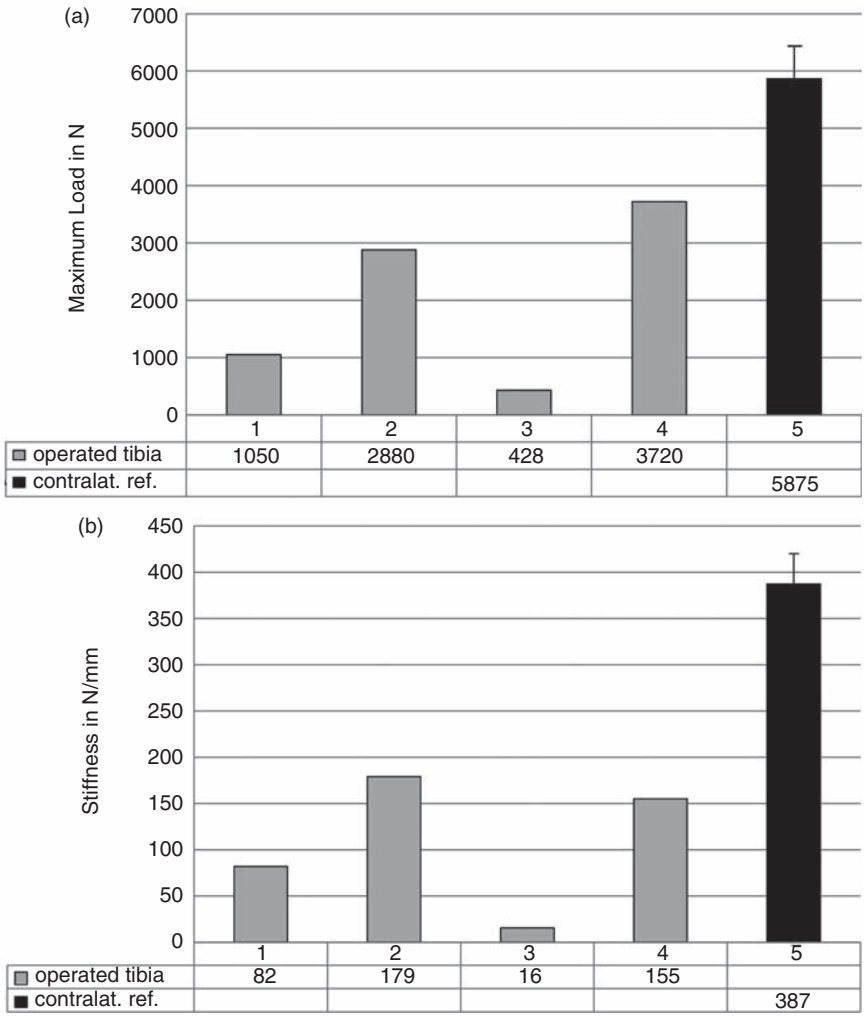

Figure 6. Biomechanical evaluation at 12 months: (a) maximum load until failure in N and (b) stiffness in N/mm. The gray bars represent the data of each animal. The black bar represents the average value of the contralateral tibiae as a reference.

months, and intermediate states of bone formation within the scaffold after 12 months (Figures 3(f) and 7(f)).

There was no inflammation or necrotic tissue detectable at both time points. The three-dimensional PCL scaffold stack did not result in any tissue defects, cysts, or non-vascularized areas after 3 or 12 months.

PCL scaffold

The coll I/CS PCL scaffold provides an appropriate network of material with interconnecting pores to act as a temporary matrix for new bone formation similar to autologous bone. Reichert et al.[32] specifies exactly these conditions for implants used in long bone engineering. Not fully interconnected and irregularly shaped pores often lead to insufficient vascularization.[43] If the pores are too small, pore blocking by the cells will happen and so inhibit cellular penetration of the inner part of the scaffolds. The triaxial structure used in this study resulted in an open porosity of 80% and in full connective micro and macropores. This allows cell penetration and proper vascularization of the scaffold. The microporosity, resulting from the coll I/CS coating ($<100\,\mu m$), should improve bone ingrowth into the scaffold by increasing the surface area for protein adsorption[44] and the vascularization.[45]

Poly(ε-caprolactone) alone has a very slow degradation rate up to 4 years, but the presence of poly(lactic acid) will accelerate the degradation.[17,46] The used PCL fiber shows a degradation rate of around 25 weeks via hydrolysis at in vitro as well as in vivo (rats, subcutaneous implantation) investigations.[18] The PCL material used in this study was still visible after 1 year of implantation. This is not surprising, given that the extent and the mechanism of the polymer hydrolysis are depending on the amount, the presence, and the location of water molecules.[46] However, it is well

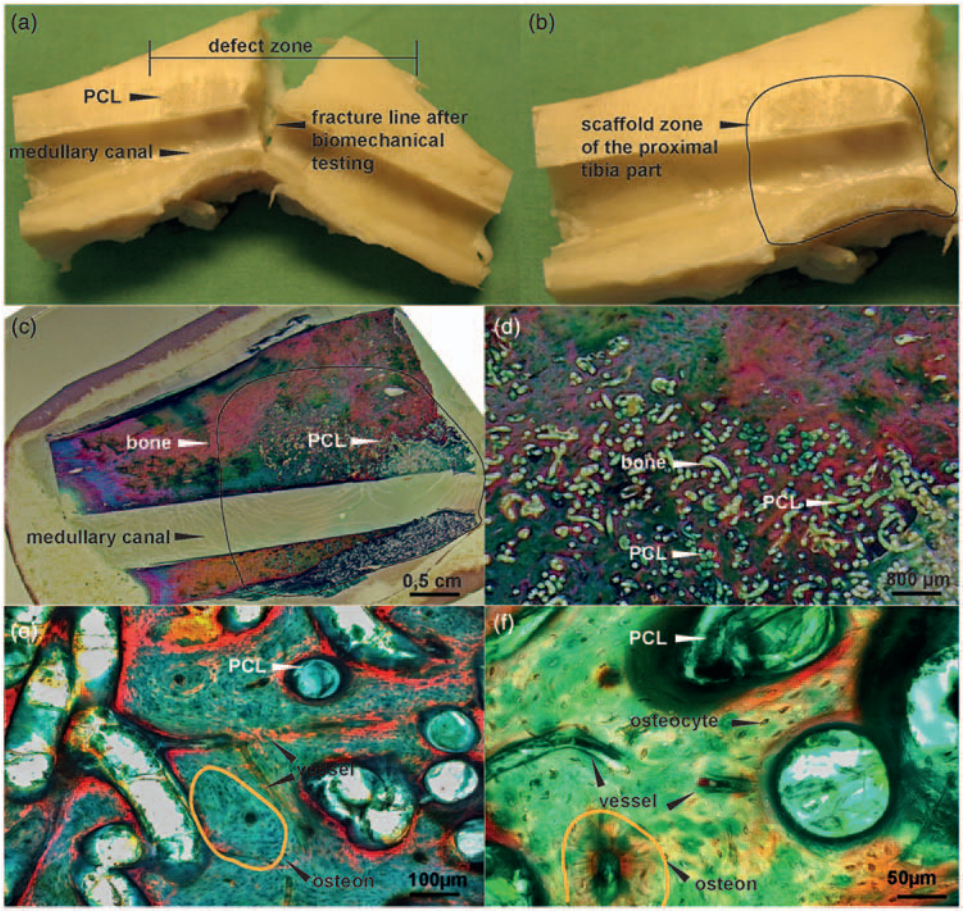

Figure 7. Histological evaluation: (a) representative picture of an explanted tibia after biomechanical testing, sectioned along the longitudinal axis by sawing, (b) implanted PCL-scaffold is marked by the black line, (c) the histological section plane is comparable with that of Figure 7(b), (d) higher magnification of Figure 7(c), the scaffold is completely intermingled with bone, (e) higher magnification of Figure 7(d) shows vessel formation within the scaffold as well as lamellar bone structures with osteons, (f) higher magnification of Figure 7(d) presenting lamellar bone structures with osteons and osteocytes and new formed blood vessels.
(c) to (f) represent Masson–Goldner trichrome staining.
PCL: polycaprolactone-co-lactide.

Table 1. Literature analysis.

Publication	Animal number/group	Animal and defect location	Defect size (cm)	Time of study (weeks)	Implant	Bone volume (%)
Anderson et al.[33]	12 animals with 24 defects, $n=6$	Goat, iliac wing	1.7	12	Empty	13.5
					Autologous bone	36.3
					Allogenic bone	18.5
					Copolymer	1.5
Arinzeh et al. and Bruder et al.[34,35]	$n=6$	Dog, femora	2.1	16	Empty	<10
					HA/βTCP	24.6
Bensaïd et al.[7]	$n=4$	Sheep, metatarsus	2.5	16	Empty	8
	$n=5$				Autologous bone	30
	$n=6$				Coral	12
	$n=7$				CHA	13

(continued)

Table 1. Continued.

Publication	Animal number/group	Animal and defect location	Defect size (cm)	Time of study (weeks)	Implant	Bone volume (%)
Kruyt et al.[36]	$n=7$	Goat, iliac wing	1.7	912	HA/TCP	10.1
	$n=8$				HA/TCP	16.7
Niemeyer et al.[37]	$n=5$	Sheep, tibia	3	26	Collagen sponge	7
Petite et al.[38]	$n=7$	Sheep, metatarsus	2.5	16	Empty	10.1
					Coral	36
Reichert et al.[39]	$n=3$	Sheep, tibiae	2	12	Empty	31.8
					Autologous bone	47.6
					PDLL–TCP–PCL	30.3
					PCL–TCP	12
Viateau et al.[9]	$n=5$	Sheep, metatarsus	2.5	24	Empty	4
	$n=6$				Autologous bone	70
	$n=4$				Coral	24
Bone volume of the empty control groups						13
Bone volume of the autologous control groups						46
Bone volume of the implant groups						17

Copolymer: polyethylene oxide/polybutylene terephthalate 70/30; HA/βTCP: hydroxyapatite/β-tricalciumphosphate (65%/35%) (Zimmer, Warsaw, IN); Coral: Bicoral (Bicoral, Levallois-Perret); CHA: coral-based hydroxyapatite (CHA/Proosteon 200R, Interpore Cross International); HA/TCP: hydroxyapatite/tricalcium phosphate (BCP, Os Satura™, IsoTis); collagene sponge (Healos, DePuy, USA); PDLL–TCP–PCL: Poly(L-lactid-co-D,L-lactide)–polycaprolactone–tricalcium phosphate; PCL–TCP: polycaprolactone–tricalcium phosphate; Coral: scaffold (Biocoral, Inc.).

accepted that a scaffold for bone reconstruction should be able to provide mechanical support up to 1 year. During this time, new bone tissue should be grown and the mechanical support of the scaffold should start to transfer back.[46]

Conclusion

This pilot study has demonstrated that embroidered and biologically modified coll I/CS PCL scaffolds provide an appropriate network of pores to permit a complete vascularization and bone tissue formation within a critical size bone defect in a preclinical large animal model. These preliminary data are encouraging for future experiments with a larger group of animals and different fixation methods.

Acknowledgments

The authors thank Möckel Embroidery and Engineering Company (Auerbach, Germany) for producing the PCL scaffolds. They also thank S. Manthey and A. Wenke for preparation and staining of the histological sections.

Conflict of interest

No benefit of any kind will be received either directly or indirectly by the authors.

Funding

The authors thank the Sächsische Aufbaubank (SAB) for financing. C. Rentsch, W. Schneiders, R. Bernhard, D. Scharnweber, and S. Rammelt are funded in part by the Deutsche Forschungsgemeinschaft, DFG (TRR 67).

References

1. Cancedda R, Giannoni P and Mastrogiacomo M. A tissue engineering approach to bone repair in large animal models and in clinical practice. *Biomaterials* 2007; 28: 4240–4250.
2. Drosse I, Volkmer E, Capanna R, et al. Tissue engineering for bone defect healing: an update on a multi-component approach. *Injury* 2008; 39: 9–20.
3. Jensen T, Jakobsen T, Baas J, et al. Hydroxyapatite nanoparticles in poly-D,L-lactic acid coatings on porous titanium implants conducts bone formation. *J Biomed Mater Res A* 2010; 95: 665–672.
4. Mihalko WM, Howard C, Dimaano F, et al. Effects of hydroxyapatite on titanium foam as a bone in growth surface in acetabular shells: a canine study. *J Long Term Eff Med Implants* 2010; 20: 35–42.
5. Rammelt S, Heck C, Bernhardt R, et al. In vivo effects of coating loaded and unloaded Ti implants with collagen, chondroitin sulfate, and hydroxyapatite in the sheep tibia. *J Orthop Res* 2007; 25: 1052–1061.

6. Zhang P, Hong Z, Yu T, et al. In vivo mineralization and osteogenesis of nanocomposite scaffold of poly(lactide-co-glycolide) and hydroxyapatite surface-grafted with poly(L-lactide). *Biomaterials* 2009; 30: 58–70.
7. Bensaïd W, Oudina K, Viateau V, et al. De novo reconstruction of functional bone by tissue engineering in the metatarsal sheep model. *Tissue Eng* 2005; 11: 814–824.
8. Sarkar MR, Augat P, Shefelbine SJ, et al. Bone formation in a long bone defect model using a platelet-rich plasma-loaded collagen scaffold. *Biomaterials* 2006; 27: 1817–1823.
9. Viateau V, Guillemin G, Bousson V, et al. Long-bone critical-size defects treated with tissue-engineered grafts: a study on sheep. *J Orthop Res* 2007; 25: 741–749.
10. Betz OB, Betz VM, Abdulazim A, et al. The repair of critical-sized bone defects using expedited, autologous BMP-2 gene-activated fat implants. *Tissue Eng Part A* 2010; 16: 1093–1101.
11. Betz VM, Betz OB, Glatt V, et al. Healing of segmental bone defects by direct percutaneous gene delivery: effect of vector dose. *Hum Gene Ther* 2007; 18: 907–915.
12. Blokhuis TJ. Formulations and delivery vehicles for bone morphogenetic proteins: latest advances and future directions. *Injury* 2009; 40: 8–11.
13. Schieker M and Mutschler W. Bridging posttraumatic bony defects: established and new methods. *Unfallchirurg* 2006; 109: 715–732.
14. Schmidt-Rohlfing B, Tzioupis C, Menzel CL, et al. Tissue engineering of bone tissue: principles and clinical applications. *Unfallchirurg* 2009; 112: 785–794.
15. Williams JM, Adewunmi A, Schek RM, et al. Bone tissue engineering using polycaprolactone scaffolds fabricated via selective laser sintering. *Biomaterials* 2005; 26: 4817–4827.
16. Rentsch C, Rentsch B, Breier A, et al. Long-bone critical-size defects treated with tissue-engineered polycaprolactone-co-lactide scaffolds: a pilot study on rats. *J Biomed Mater Res A* 2010; 95: 964–972.
17. Bramfeldt H, Sarazin P and Vermette P. Chracterization, degradation, and mechanical strength of poly(D,L-lactide-co-ε-caprolactone)-poly(ethylene glycol)-poly(D,L-lactide-co-ε-caprolactone). *J Biomed Mater Res A* 2007; 83: 503–511.
18. Tomihata K, Suzuki M, Oka T, et al. A new resorbable monofilament suture. *Polymer Degrad Stabil* 1998; 51: 13–18.
19. Rammelt S, Schulze E, Witt M, et al. Collagen type I increases bone remodelling around hydroxyapatite implants in the rat tibia. *Cells Tissues Organs* 2004; 178(3): 146–157.
20. Morra M, Cassinelli C, Meda L, et al. Surface analysis and effects on interfacial bone microhardness of collagen-coated titanium implants: a rabbit model. *Int J Oral Maxillofac Implants* 2005; 20(1): 23–30.
21. Rammelt S, Illert T, Bierbaum S, et al. Coating of titanium implants with collagen, RGD peptide and chondroitin sulfate. *Biomaterials* 2006; 27: 5561–5571.
22. Rentsch B, Hofmann A, Breier A, et al. Embroidered and surface modified polycaprolactone-co-lactide scaffolds as bioartificial bone substitute: in vitro characterization. *Ann Biomed Eng* 2009; 37: 2118–2128.
23. Schneiders W, Reinstorf A, Biewener A, et al. In vivo effects of modification of hydroxyapatite/collagen composites with and without chondroitin sulphate on bone remodeling in the sheep tibia. *J Orthop Res* 2009; 27: 15–21.
24. Stadlinger B, Bierbaum S, Grimmer S, et al. Increased bone formation around coated implants. *J Clin Periodontol* 2009; 36: 698–704.
25. Wollenweber M, Domaschke H, Hanke T, et al. Mimicked bioartificial matrix containing chondroitin sulphate on a textile scaffold of poly(3-hydroxybutyrate) alters the differentiation of adult human mesenchymal stem cells. *Tissue Eng* 2006; 12: 345–359.
26. Rentsch C, Rentsch B, Breier A, et al. Evaluation of the osteogenic potential and vascularization of 3D poly(3)hydroxybutyrate scaffolds subcutaneously implanted in nude rats. *J Biomed Mater Res A* 2010; 92: 185–195.
27. Masquelet AC. Muscle reconstruction in reconstructive surgery: soft tissue repair and long bone reconstruction. *Langenbecks Arch Surg* 2003; 388(5): 344–346.
28. Biewener A, Meyer J, Rentsch C, et al. Internal fixation of meta- and diaphyseal intercalary bone defects after tumour resection with intramedullary nailing and porous polymethylmetacrylate (PMMA) spacer. *Orthopade* 2007; 36: 152–158, 160–163.
29. Nafei A, Danielsen CC, Linde F, et al. Properties of growing trabecular ovine bone. Part I: mechanical and physical properties. *J Bone Joint Surg Br* 2000; 82: 910–920.
30. Regauer M, Jürgens I, Kotsianos D, et al. New-bone formation by osteogenic protein-1 and autogenic bone marrow in a critical tibial defect model in sheep. *Zentralbl Chir* 2005; 130: 338–345.
31. Reichert JC, Epari DR, Wullschleger ME, et al. Establishment of a preclinical ovine model for tibial segmental bone defect repair by applying bone tissue engineering strategies. *Tissue Eng Part B* 2010; 16: 93–104.
32. Hahn JA, Witte TS, Arens D, et al. Double-plating of ovine critical sized defects of the tibia: a low morbidity model enabling continuous in vivo monitoring of bone healing. *BMC Musculoskelet Disord* 2011; 12: 214.
33. Anderson ML, Dhert WJ, de Bruijn JD, et al. Critical size defect in the goat's os ilium: a model to evaluate bone grafts and substitutes. *Clin Orthop Relat Res* 1999; 364: 231–239.
34. Arinzeh TL, Peter SJ, Archambault MP, et al. Allogeneic mesenchymal stem cells regenerate bone in a critical-sized canine segmental defect. *J Bone Joint Surg Am* 2003; 85–A: 1927–1935.
35. Bruder SP, Kraus KH, Goldberg VM, et al. The effect of implants loaded with autologous mesenchymal stem cells on the healing of canine segmental bone defects. *J Bone Joint Surg Am* 1998; 80: 985–996.
36. Kruyt MC, Dhert WJ, Yuan H, et al. Bone tissue engineering in a critical size defect compared to ectopic implantations in the goat. *J Orthop Res* 2004; 22: 544–551.

37. Niemeyer P, Fechner K, Milz S, et al. Comparison of mesenchymal stem cells from bone marrow and adipose tissue for bone regeneration in a critical size defect of the sheep tibia and the influence of platelet-rich plasma. *Biomaterials* 2010; 31: 3572–3579.
38. Petite H, Viateau V, Bensaïd W, et al. Tissue-engineered bone regeneration. *Nat Biotechnol* 2000; 18: 959–963.
39. Reichert JC, Wullschleger ME, Cipitria A, et al. Custom-made composite scaffolds for segmental defect repair in long bones. *Int Orthop* 2011; 35(8): 1229–1236.
40. Mastrogiacomo M, Corsi A, Francioso E, et al. Reconstruction of extensive long bone defects in sheep using resorbable bioceramics based on silicon stabilized tricalcium phosphate. *Tissue Eng* 2006; 12(5): 1261–1273.
41. Mittra E, Rubin C and Qin YX. Mittra interrelationship of trabecular mechanical and microstructural properties in sheep trabecular bone. *J Biomech* 2005; 38(6): 1229–1237.
42. Schindeler A, McDonald MM, Bokko P, et al. Bone remodeling during fracture repair: the cellular picture. *Semin Cell Dev Biol* 2008; 19: 459–466.
43. Hutmacher DW, Schantz T, Zein I, et al. Mechanical properties and cell cultural response of polycaprolactone scaffolds designed and fabricated via fused deposition modeling. *J Biomed Mater Res* 2001; 55(2): 203–216.
44. Woodard JR, Hilldore AJ, Lan SK, et al. The mechanical properties and osteoconductivity of hydroxyapatite bone scaffolds with multi-scale porosity. *Biomaterials* 2007; 28(1): 45–54.
45. Rezwan K, Chen QZ, Blaker JJ, et al. Biodegradable and bioactive porous polymer/inorganic composite scaffolds for bone tissue engineering. *Biomaterials* 2006; 27(18): 3413–3431.
46. Lam CX, Savalani MM, Teoh SH, et al. Dynamics of in vitro polymer degradation of polycaprolactone-based scaffolds: accelerated versus simulated physiological conditions. *Biomed Mater* 2008; 3(3): 034108.